International Journal of Biological Macromolecules 265 (2024) 130962

Contents lists available at ScienceDirect

International Journal of Biological Macromolecules

journal homepage: www.elsevier.com/locate/ijbiomac

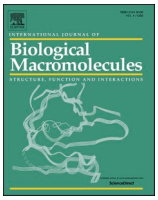

Metabolic effects of SGLT2i and metformin on 3-hydroxybutyric acid and lactate in db/db mice

Makoto Harada [a,b], Siyu Han [a,b,c], Mengya Shi [a,b,c], Jianhong Ge [a,b,c], Shixiang Yu [a,c], Jonathan Adam [d], Jerzy Adamski [e,f,g], Markus F. Scheerer [e], Susanne Neschen [e], Martin Hrabe de Angelis [b,e,h], Rui Wang-Sattler [a,b,*]

[a] Institute of Translational Genomics, Helmholtz Zentrum München - German Research Center for Environmental Health, Neuherberg, Germany
[b] German Center for Diabetes Research (DZD), München-Neuherberg, Germany
[c] School of Medicine, Technical University of Munich (TUM), Munich, Germany
[d] Institute of Epidemiology, Helmholtz Zentrum München - German Research Center for Environmental Health, Neuherberg, Germany
[e] Institute of Experimental Genetics, Helmholtz Zentrum München - German Research Center for Environmental Health, Neuherberg, Germany
[f] Department of Biochemistry, Yong Loo Lin School of Medicine, National University of Singapore, Singapore
[g] Institute of Biochemistry, Faculty of Medicine, University of Ljubljana, 1000 Ljubljana, Slovenia
[h] Chair of Experimental Genetics, School of Life Sciences, Technical University of Munich (TUM), Freising, Germany

ARTICLE INFO

Keywords:
Diabetic ketoacidosis
Lactic acidosis
SGLT2i monotherapy
Metformin adds to SGLT2i
Branched-chain amino acids

ABSTRACT

Combining a Sodium-Glucose-Cotransporter-2-inhibitor (SGLT2i) with metformin is recommended for managing hyperglycemia in patients with type 2 diabetes (T2D) who have cardio-renal complications. Our study aimed to investigate the metabolic effects of SGLT2i and metformin, both individually and synergistically. We treated leptin receptor-deficient (db/db) mice with these drugs for two weeks and conducted metabolite profiling, identifying 861 metabolites across kidney, liver, muscle, fat, and plasma. Using linear regression and mixed-effects models, we identified two SGLT2i-specific metabolites, X-12465 and 3-hydroxybutyric acid (3HBA), a ketone body, across all examined tissues. The levels of 3HBA were significantly higher under SGLT2i monotherapy compared to controls and were attenuated when combined with metformin. We observed similar modulatory effects on metabolites involved in protein catabolism (e.g., branched-chain amino acids) and gluconeogenesis. Moreover, combination therapy significantly raised pipecolate levels, which may enhance mTOR1 activity, while modulating GSK3, a common target of SGLT2i and 3HBA inhibition. The combination therapy also led to significant reductions in body weight and lactate levels, contrasted with monotherapies. Our findings advocate for the combined approach to better manage muscle loss, and the risks of DKA and lactic acidosis, presenting a more effective strategy for T2D treatment.

1. Introduction

Type 2 diabetes (T2D) is a heterogeneous disease, which is associated with complications such as cardiovascular and kidney diseases (also termed cardio-renal diseases) [1,2]. Besides the strong hereditary component [3], the development of T2D is mainly caused by unhealthy lifestyles (e.g., physical inactivity) and excessive dietary intake [4]. The drug treatment is an important component for the management of T2D, in addition to the improvements of lifestyles and dietary habits [1,5]. According to the current trend and consensus on drug treatment for patients with T2D, metformin and sodium-glucose-cotransporter-2-inhibitor (SGLT2i) are highly recommended: 70 % to 90 % of patients with T2D have been prescribed metformin as first-line therapy worldwide [6–8]. Then, SGLT2i is added to metformin as a combination therapy for better glycemic control and to decrease cardiorenal risk [1,7]. The cardiorenal-protective effect of SGLT2i is considered to be achieved through the blockage of SGLT2 in the proximal tubules of the kidney, enhancing the excretion of glucose from the circulating blood into the urine, along with associated metabolic mechanisms [9]. However, the use of SGLT2i could also cause the progression of fatty acid

* Corresponding author at: Institute of Translational Genomics, Helmholtz Zentrum München - German Research Center for Environmental Health, Neuherberg, Germany.
E-mail address: rui.wang-sattler@helmholtz-munich.de (R. Wang-Sattler).

https://doi.org/10.1016/j.ijbiomac.2024.130962
Received 6 September 2023; Received in revised form 15 March 2024; Accepted 15 March 2024
Available online 17 March 2024

oxidation and ketogenesis due to the glucose loss resulting in diabetic ketoacidosis (DKA), which is a life-threatening complication of diabetes [10]. In addition, SGLT2i may lead to the loss of skeletal muscles [11,12]. To investigate mechanisms of the cardiorenal-protective effects on SGLT2i, metabolomics studies have been performed with serum samples from patients with T2D and cardiovascular disease ($N = 25$), as well as from mice [13,14]. However, metabolic changes in multiple organs, particularly in muscles, induced by SGLT2i monotherapy and its combination therapy with metformin, have not been investigated. Moreover, while metformin is associated with a risk of lactic acidosis, it is important to note that this is a rare but serious medical condition, which is of particular concern in patients with kidney disease [15,16]. Therefore, in pursuit of cardiorenal protective benefits and the reduction of risk such as DKA and muscle loss associated with SGLT2i, as well as lactic acidosis with metformin, it is essential to understand pathophysiological pathways influenced by each drug and their combined regimen [17].

Herein, we investigate the metabolomic differences and relationships in five tissues (kidney, liver, muscle, fat, and plasma) using untargeted metabolomics data of leptin receptor-deficient (db/db) mice treated with different regimens: vehicle-gavaged (VG) as the control, SGLT2i as monotherapy (SGLT2i), SGLT2i and metformin as the combination therapy (SGLT2i + MET), and metformin monotherapy (MET) for a two-week duration. We further identify the organ-specific metabolic pathways of monotherapy (SGLT2i), and the combination therapy in order to better understand the underlying pathophysiological mechanisms.

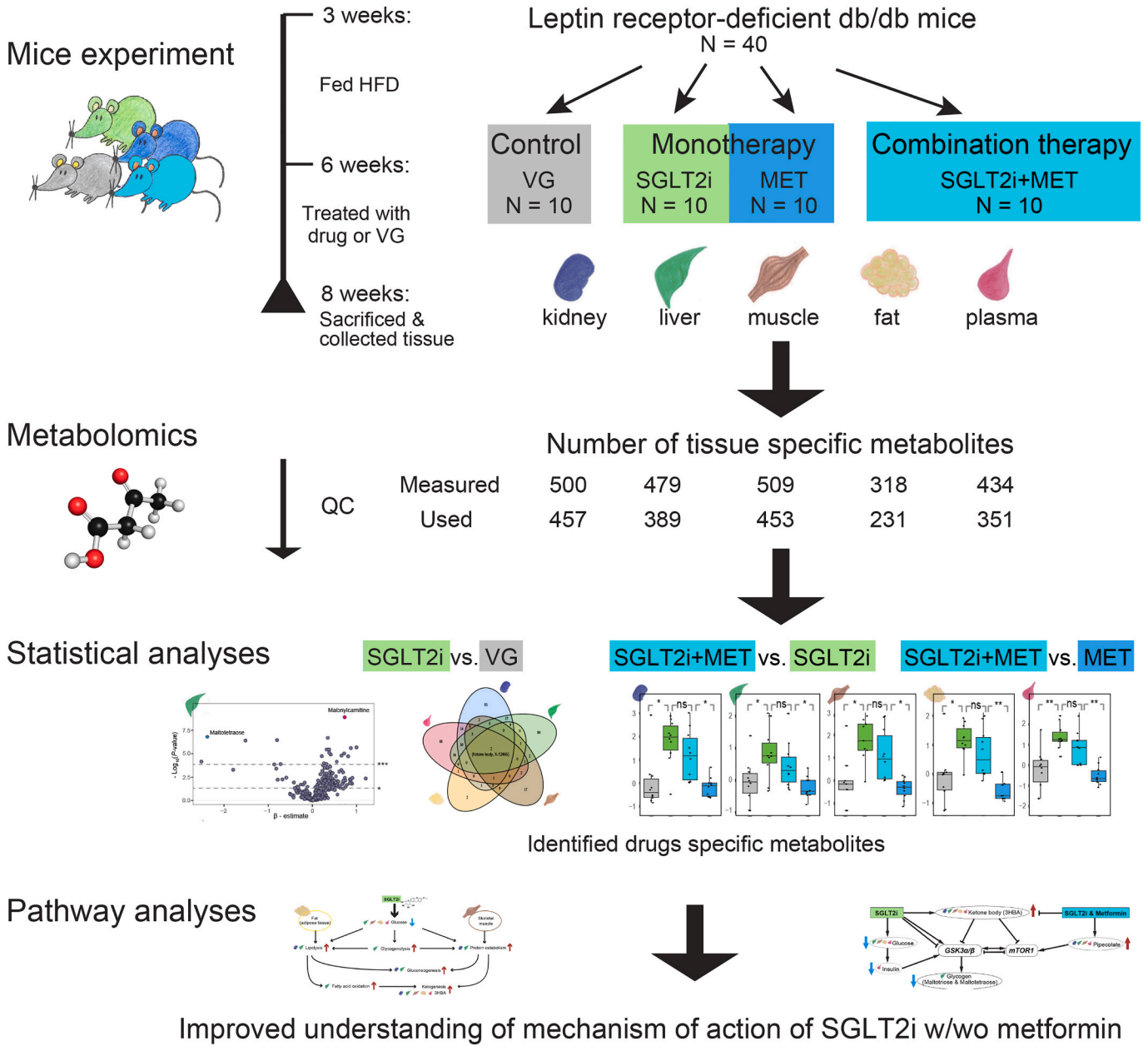

Fig. 1. Study design.
The study flow started with the mice experiment, and performed metabolomics analyses with collected tissues, continued with statistical and pathway analyses. Abbreviations: HFD, high-fat diet; QC, quality control; MET, metformin-treated db/db mice; SGLT2i, SGLT2 inhibitor-treated db/db mice; SGLT2i + MET, SGLT2i and metformin-treated db/db mice; VG, vehicle-gavaged db/db mice; w/wo, with or without.

2. Materials and method

2.1. Study design

The flow of this study is shown in Fig. 1. We first conducted the mice experiment ($N = 40$) and collected tissue samples (kidney, liver, muscle, fat, and plasma) for each mouse after two weeks of treatment (VG, or drugs). Second, we performed untargeted metabolomics analyses for each collected sample of each mouse. After tissue-specific quality control (QC) and imputation of missing data, we statistically analyzed the metabolomics data and performed pairwise comparisons to examine the impact of monotherapy and the combination therapy (e.g., SGLT2i vs. VG, SGLT2i + MET vs. SGLT2i, and SGLT2i + MET vs. MET). Third, the relevance of the identified drug-specific metabolites was further investigated with tissue-specific pathway analyses. The details were described below in each section, respectively.

2.2. Animal experiment

We performed the mice study using the C57BL6-based BKS.Cg-Dock^{7m}+/+ Lepr^{db}/J db/db mice, which is a common murine model of T2D. The mice were maintained in a specific pathogen-free facility and housed in a light- and temperature-controlled environment in compliance with FELASA (the Federation of Laboratory Animal Science Associations) protocols. Animal experiments were approved by the Upper Bavarian government (Gz.55.2–1-54-2531-70-07, 55.2-1-2532-153-11). Only male mice were included in this study. At the age of 3 weeks, mice were started feeding on a high-fat diet (HFD, Ssniff Spezialdiäten, Soest, Germany). Contents of HFD were as follows: palm fat (13.5 % of fat), sunflower oil (13.5 %), starch (30 %), saccharose (10 %), casein (20 %), lignocellulose (5 %), mineral plus vitamin mix (5 and 2 %, respectively), safflower oil (0.5 %), and linseed oil (0.5 %). From age 6 weeks (termed as 'start', Table 1), mice were randomly divided into four groups: 1) treated with vehicle (5 % solutol and 95 % hydroxyethylcellulose, VG, $N = 10$); 2) treated with SGLT2i (AVE2268, 30 mg/kg; Sanofi AG, Frankfurt, Germany [18], SGLT2i, $N = 10$); 3) treated with SGLT2i (AVE2268, 30 mg/kg; Sanofi AG, Frankfurt, Germany) and metformin (300 mg/kg; Sigma Aldrich, Taufkirchen, Germany) (SGLT2i + MET, N = 10); 4) treated with metformin (300 mg/kg; Sigma Aldrich, Taufkirchen, Germany) (MET, N = 10). All mice treatment was performed via gavage once daily between 5:00 and 6:00 P.M. before dark-phase onset (6:00 P.M.) for 14 days (i.e., age 8 weeks, termed as 'end', Table 1). After 4 h from the last treatment (i.e., 4-h fasting) mice were sacrificed with an isoflurane overdose, and the kidney, liver, muscle (skeletal muscle tissue), fat (epididymal adipose tissue), and blood were immediately collected. Plasma sample was prepared from whole blood by centrifugation at 4 °C, and the other tissues were freeze-clamped. All samples were stored at −80 °C until further analyses. Details of the mice study are described in previous studies [19–21].

2.3. Untargeted metabolomic analyses and quality control

All samples (each collected tissue of each mouse) were measured with the untargeted Metabolon analytical platform (Metabolon Inc., Durham, North Carolina, USA). Metabolon applied a semiquantitative liquid chromatography–tandem mass spectrometry (LC-MS/MS) and gas chromatography–mass spectrometry (GC–MS) platform for the identification of structurally named and unknown small molecules [22,23]. We performed QC for each tissue and applied the same criteria as previously described [24,25]. In brief, metabolites with >20 % missing values were excluded, as were samples with >10 % missing metabolites [24]. All normalized relative ion counts were log-transformed, and the remaining data were imputed with Multivariate Imputation by Chained Equations (MICE) [26]. Of 1054 metabolites measured across five murine tissues, 861 metabolites passed QC. This resulted in 457, 389, 453, 231, and 351 metabolites in the kidney, liver, muscle, fat, and plasma, respectively.

2.4. Statistical analyses

We conducted pairwise linear regression analysis with the relative metabolite concentration values as outcome and the grouping variables as predictor [27]. For example, for the comparison between SGLT2i and VG mice, mice treated with SGLT2i were defined as 1, whereas control mice (VG) were assigned as 0. Each metabolite was assessed individually. Pairwise linear regression analyses were performed for each

Table 1
Characteristics of four db/db mice groups.

Clinical variables		VG	*P*-value[a]	SGLT2i	*P*-value[b]	SGLT2i + MET	*P*-value[c]	MET
Blood glucose (mg/dL)	Start (6w)	443 ± 65	0.52	461 ± 58	0.44	439 ± 62	0.57	455 ± 60
	End (8w)	422 ± 41	<0.001	163 ± 32	0.21	130 ± 46	<0.001	323 ± 93
Insulin (μg/L)	Start (6w)	7.2 ± 3.0	0.98	7.2 ± 2.4	0.54	8.0 ± 3.8	0.27	6.5 ± 2.6
	End (8w)	7.8 ± 2.3	0.06	6.0 ± 1.4	0.38	6.8 ± 2.4	0.23	7.9 ± 1.7
Lactate (mmol/L)	Start (6w)	5.9 ± 1.7	0.78	5.7 ± 0.9	0.71	5.5 ± 0.9	0.87	5.4 ± 0.7
	End (8w)	8.8 ± 2.3	0.11	7.5 ± 1.2	0.88	7.4 ± 0.9	0.11	8.5 ± 1.2
Body weight (g)	Start (6w)	49.2 ± 2.8	0.78	49.6 ± 2.5	0.48	48.8 ± 2.2	0.88	48.9 ± 2.2
	End (8w)	47.9 ± 2.4	0.29	46.8 ± 2.2	1.00	46.8 ± 1.7	0.26	47.8 ± 2.1
Kidney weight (g)	End (8w)	0.20 ± 0.02	0.34	0.22 ± 0.03	0.77	0.21 ± 0.02	0.87	0.21 ± 0.02
Liver weight (g)	End (8w)	2.56 ± 0.30	0.005	2.25 ± 0.10	0.18	2.36 ± 0.19	0.006	2.61 ± 0.09

Clinical variables are shown as mean and standard deviation. The pairwise comparisons were performed by Student's *t*-test. A *P*-value <0.05 was considered statistically significant (shown in bold). Abbreviations: VG, vehicle-gavaged db/db mice ($N = 10$); SGLT2i, SGLT2i-treated db/db mice (N = 10); SGLT2i + MET, SGLT2i and metformin-treated db/db mice (N = 10); MET, metformin-treated db/db mice (N = 10); 6w, 6 weeks; 8w, 8 weeks.

[a] Compared SGLT2i with VG.

[b] Compared SGLT2i + MET with SGLT2i.

[c] Compared SGLT2i + MET with MET.

metabolite value (SGLT2 vs. VG, SGLT2 + MET vs. SGLT2i, and SGLT2i + MET vs. MET). To account for multiple testing for the linear models, Bonferroni correction was first applied, this led to P-value $<0.05/457 = 1.09 \times 10^{-4}$ for the kidney, P-value $<0.05/389 = 1.29 \times 10^{-4}$ for the liver, P-value $<1.10 \times 10^{-4}$ for the muscle, P-value $<2.16 \times 10^{-4}$ for the fat, and P-value $<0.05/351 = 1.42 \times 10^{-4}$ for the plasma. Furthermore, metabolites with P-value <0.05 were considered to be statistically significantly different.

For clinical variables, we pairwise compared the values among four db/db mice groups using Student's t-test (SGLT2 vs. VG, SGLT2 + MET vs. SGLT2i, and SGLT2i + MET vs. MET). To evaluate the changes of clinical phenotypes during the two week treatment, linear mixed effects models were used.

All statistical analyses were performed in R (version 4.1.2).

2.5. Pathway analyses

Pathways analyses were performed using databases, such as the Human Metabolome Database [28], and the Kyoto Encyclopedia of Genes and Genomes [29], by considering tissue and organ specificity in addition to literature research.

2.6. Data and resource availability

The data sets generated and/or analyzed during the current study are available from the corresponding author upon reasonable request.

3. Results

3.1. Characteristics of mouse groups

All four groups of db/db mice studied here (VG, SGLT2i, SGLT2i + MET, and MET) had comparable values of blood glucose, insulin, lactate, and body weight at the start (i.e. pre-treatment, 6 weeks, Table 1). After two weeks of treatment with vehicle and drugs, the mice with the post-treatment (8 weeks) experienced a reduction in blood glucose levels of approximately 21, 298, 309, and 132 mg/dL for the VG, SGLT2i, SGLT2i + MET and MET groups, respectively (Table 2). We observed similar reductions in body weight of approximately 1.4 g in VG, 2.8 g in SGLT2i, 2.0 g in SGLT2i + MET, and 1.1 g in MET groups. Since the reductions were also observed in the control group, we further pairwise evaluated these changes using linear mixed effects models. We found significant (P-value <0.05) reduction in blood glucose, insulin, and body weight when comparing SGLT2i with the control VG mice. Moreover, the combination therapy significantly decreased body weight compared to that in SGLT2i monotherapy (Table 2). When comparing the combination therapy with metformin monotherapy (SGLT2i + MET vs. MET), we observed significant decreases in blood glucose, insulin, and body weight, along with an increase in lactate level between post-treatment and pre-treatment (Table 2).

3.2. Identification of SGLT2i-specific metabolites in five tissues

To identify metabolites altered by SGLT2i monotherapy, we conducted pairwise comparisons between the SGLT2i group and the VG control across each tissue using linear regression analysis. Significant changes in metabolite profiles were observed. Specifically, in the kidney, 113 metabolites significantly altered (P-value <0.05), with 6 meeting the Bonferroni correction threshold (P-value $<1.09 \times 10^{-4}$, Fig. 2A). In the liver, muscle, fat, and plasma, there were 136, 31, 8, and 138 significantly changed metabolites, respectively, with 18 in the liver, 2 in the muscle, 1 in fat, and 17 in plasma also reaching Bonferroni significance (Fig. 2A). Notably, two metabolites, 3-hydroxybutyric acid (3HBA, a ketone body) and an unidentified compound designated as metabolite X-12465, were found at consistently higher levels in the SGLT2i group compared to VG across all five tissues (Fig. 2B, Table S1).

In the liver of SGLT2i-treated mice compared to VG controls, we observed a significant reduction in glycogenolysis-related metabolites, such as maltotriose and maltotetraose (Fig. 3A, Table S2). Conversely, significantly higher levels of metabolites associated with the fatty acid oxidation pathway, including malonylcarnitine and acetylcarnitine, as well as free fatty acids-related metabolites (e.g., laurate, myristate, palmitate, and oleate) were observed (Fig. 3B, Table S3). In the kidneys, SGLT2i treatment correlated with elevated levels of metabolites in the lipolysis pathway, including glycerol, glycerol-2-phosphate and glycerol-3-phosphate (Table S3).

Across multiple tissues, the comparison between SGLT2i-treated mice and VG controls revealed a consistent elevation in metabolites involved in protein metabolism. Notably, the branched-chain amino acids (BCAAs) such as leucine, isoleucine, and valine were significantly higher in the kidney, liver, muscle, and plasma (Fig. 4, Table S4). The plasma also showed significant higher levels in BCAA catabolites, including isovalerylglycine and 3-methyl-2-oxovalerate, in the SGLT2i group.

Our observations also revealed a metabolic profile consistent with the clinically observed lower blood glucose levels in SGLT2i-treated mice when compared to VG controls (Table 1). In line with these clinical observations, glucose levels were significantly lower in the liver, muscle, and fat tissues of the SGLT2i group (Fig. 3C, Table S5). On the other hand, the kidneys of SGLT2i-treated mice exhibited a higher level in metabolites associated with gluconeogenesis, such as phosphoenolpyruvate, 2-phosphoglycerate, and 3-phosphoglycerate, indicating a tissue-specific response to the treatment (Table S5).

Table 2
Pairwise comparison of phenotypic changes of db/db mice groups between the two weeks treatment.

Clinical variables	VG	P-value [a]	SGLT2i	P-value [b]	SGLT2i + MET	P-value [c]	MET
Changed blood glucose (mg/dL)	−21 (49)	<0.001	−298 (51)	0.57	−309 (37)	<0.001	−132 (66)
Changed insulin (μg/L)	0.5 (1.9)	0.049	−1.2 (1.8)	0.97	−1.2 (2.7)	0.018	1.3 (1.6)
Changed lactate (mmol/L)	3.0 (1.9)	0.17	1.8 (1.8)	0.90	1.8 (0.9)	0.013	3.0 (1.0)
Changed body weight (g)	−1.4 (0.7)	<0.001	−2.8 (0.6)	0.009	−2.0 (0.6)	<0.001	−1.1 (0.2)

Clinical variables are shown as changed mean and standard deviation between post-treatment (8 weeks) and pre-treatment (6 weeks). The changes between two groups were evaluated with the linear mixed effects models. A P-value <0.05 was considered statistically significant (shown in bold). Abbreviations: VG, vehicle-gavaged db/db mice; SGLT2i, SGLT2i-treated db/db mice; SGLT2i + MET, SGLT2i and metformin-treated db/db mice; MET, metformin-treated db/db mice.

[a] Compared SGLT2i with VG.

[b] Compared SGLT2i + MET with SGLT2i.

[c] Compared SGLT2i + MET with MET.

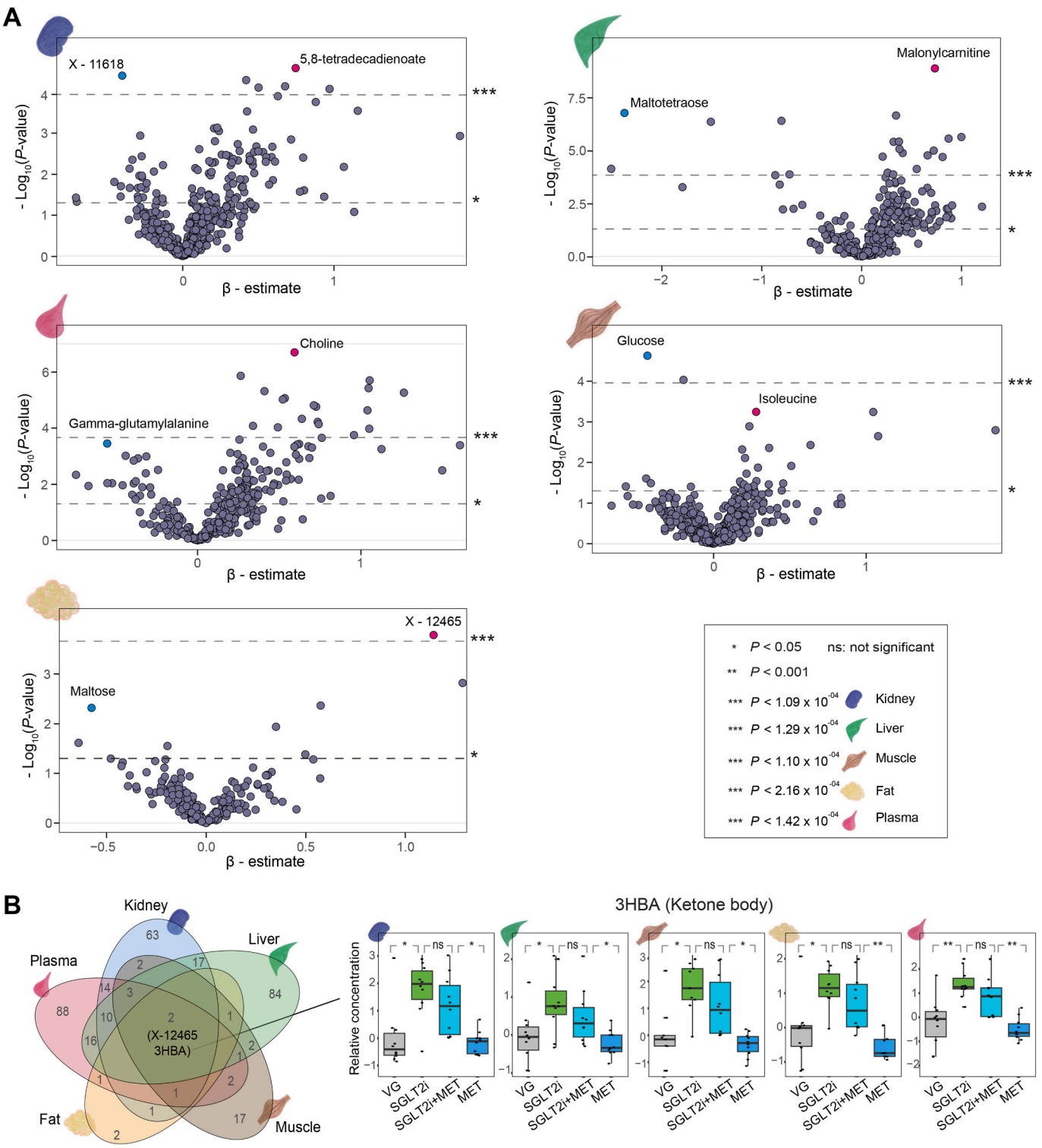

Fig. 2. Identification and comparisons of SGLT2i-specific metabolites in SGLT2i and VG mice.
(A) Identification of SGLT2i-specific metabolites in 5 tissues. Volcano plots of metabolites analyzed by linear regression analysis for the kidney, liver, muscle, fat, and plasma comparing SGLT2i to VG mice (β-estimates and *P*-values). Metabolites that have positive and negative β-estimates with top *P*-value are presented in red and blue dots, respectively. The upper and lower dashed lines represent Bonferroni-corrected and uncorrected (*P*-value = 0.05) significance levels, respectively. (B) Number of overlapped significant metabolites, and comparisons of the relative concentration of X-12465 presented as boxplots in the kidney, liver, muscle, fat, and plasma between SGLT2i and VG mice. Abbreviations: SGLT2i, SGLT2 inhibitor-treated db/db mice; VG, vehicle-gavaged db/db mice.

3.3. Identification of tissue-specific metabolites for the combination therapy

To identify metabolites uniquely altered by combination therapy with SGLT2i and metformin, we compared the SGLT2i + MET group to the SGLT2i monotherapy group across all five tissues. We found that 63, 45, 27, 17, and 47 metabolites were significantly altered (*P*-value <0.05) in kidney, liver, muscle, fat, and plasma, respectively (Fig. 5B).

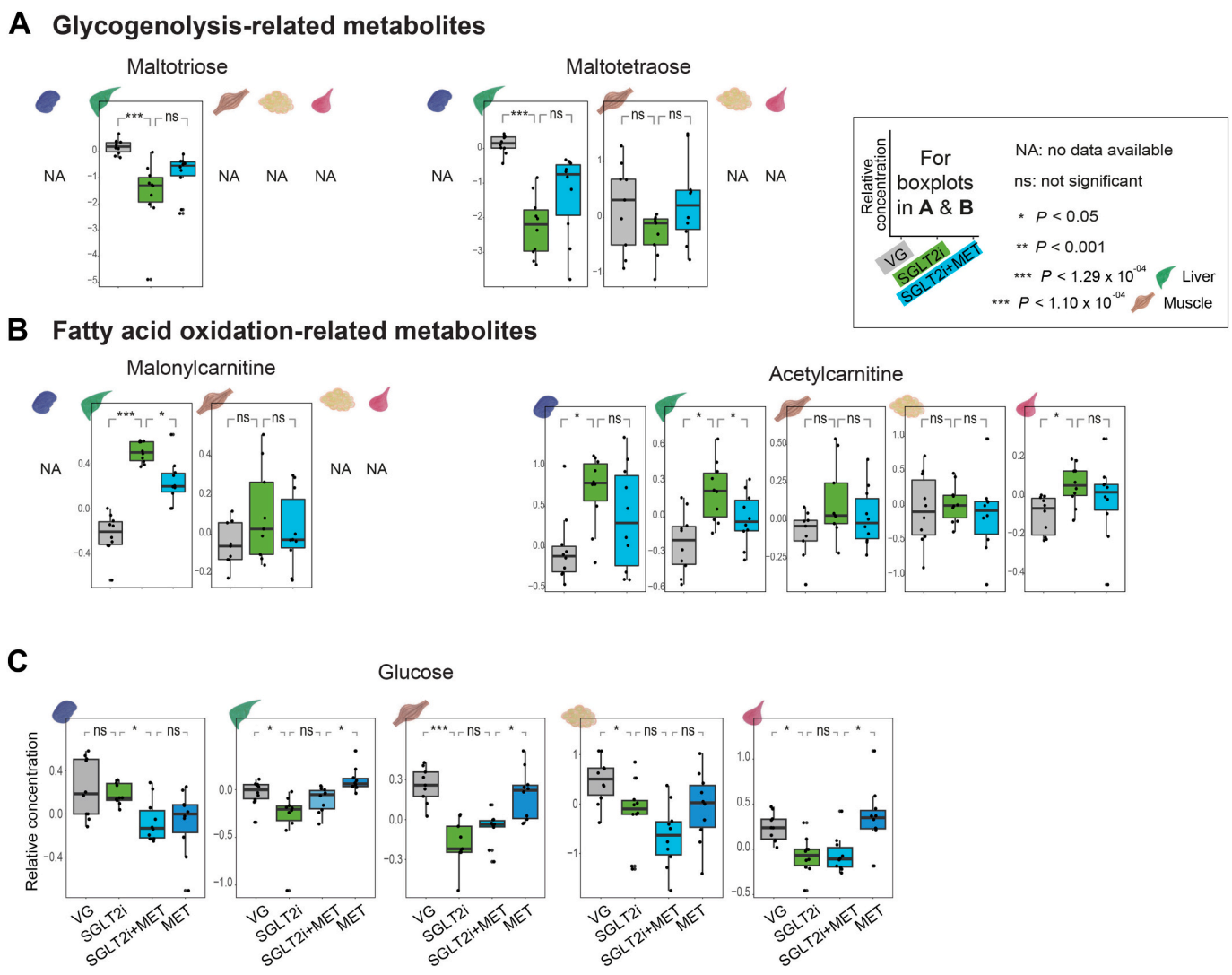

Fig. 3. Glycogenolysis and fatty acid oxidation related metabolites.
Comparisons of the relative concentration of selected metabolites presented as boxplots in the kidney, liver, muscle, fat, and plasma among VG, SGLT2i, SGLT2i + MET and MET groups. Abbreviations: NA, not available; ns; not significant; SGLT2i, SGLT2 inhibitor-treated db/db mice; SGLT2i + MET, SGLT2 inhibitor and metformin combination-treated db/db mice; VG, vehicle gavaged db/db mice, MET, metformin treated db/db mice.

For instance, pipecolate levels were significantly higher in the SGLT2i + MET group compared to the SGLT2i group in the kidney, liver, muscle, and plasma (Table S4). While the ketone body showed no significant differences, their relative concentrations were generally lower in the SGLT2i + MET group across all tissues examined (Fig. 2B, Table S1).

In terms of glycogenolysis, the metabolite levels were similar when comparing combination therapy to SGLT2i monotherapy. However, metabolites in the fatty acid oxidation pathway, such as malonylcarnitine and acetylcarnitine in the liver, and key gluconeogenesis intermediates like glucose, phosphoenolpyruvate, and 3-phosphoglycerate in the kidneys, were significantly lower under the combination therapy (Fig. 3A, B, C, Tables S2, S3, S5). Furthermore, combination therapy resulted in lower levels of various metabolites related to protein catabolism. This included reductions in leucine in the kidneys; valine in the liver, muscle, fat, and plasma; and leucine, isoleucine, and isovalerylglycine in the plasma when compared to SGLT2i monotherapy (Fig. 4, Table S4).

In a subsequent analysis, we compared the effects of combination therapy with metformin monotherapy. Notably, levels of 3HBA were significantly elevated in the combination therapy group across all five tissues examined (Fig. 2B, Table S1). Additionally, plasma levels of glucose, lactate, and pyruvate were significantly lower in the SGLT2i + MET group compared to the MET group (Fig. 3C, Table S5), aligning with the clinical phenotypic changes between the two weeks treatment for both glucose and lactate (Table 2).

4. Discussion and conclusion

In our comprehensive study, we assessed the phenotypic and metabolic consequences of SGLT2i both as a monotherapy and in conjunction with metformin in four groups of db/db mice. This was facilitated by analysis of 861 metabolites across five tissues, kidney, liver, muscle, fat, and plasma. Our findings indicated that SGLT2i monotherapy prominently amplified several metabolic pathways, such as lipolysis, glycogenolysis, protein catabolism, gluconeogenesis, fatty acid oxidation, and notably, ketogenesis, with the liver showing particularly heightened activity (Fig. 5A).

We then observed that the dual regimen of SGLT2i and metformin markedly mitigated the activity within the protein catabolism and gluconeogenesis pathways, most notably within the renal tissue (Fig. 5C). This suggests that the combination therapy not only counterbalances the potential adverse effects of SGLT2i monotherapy, such

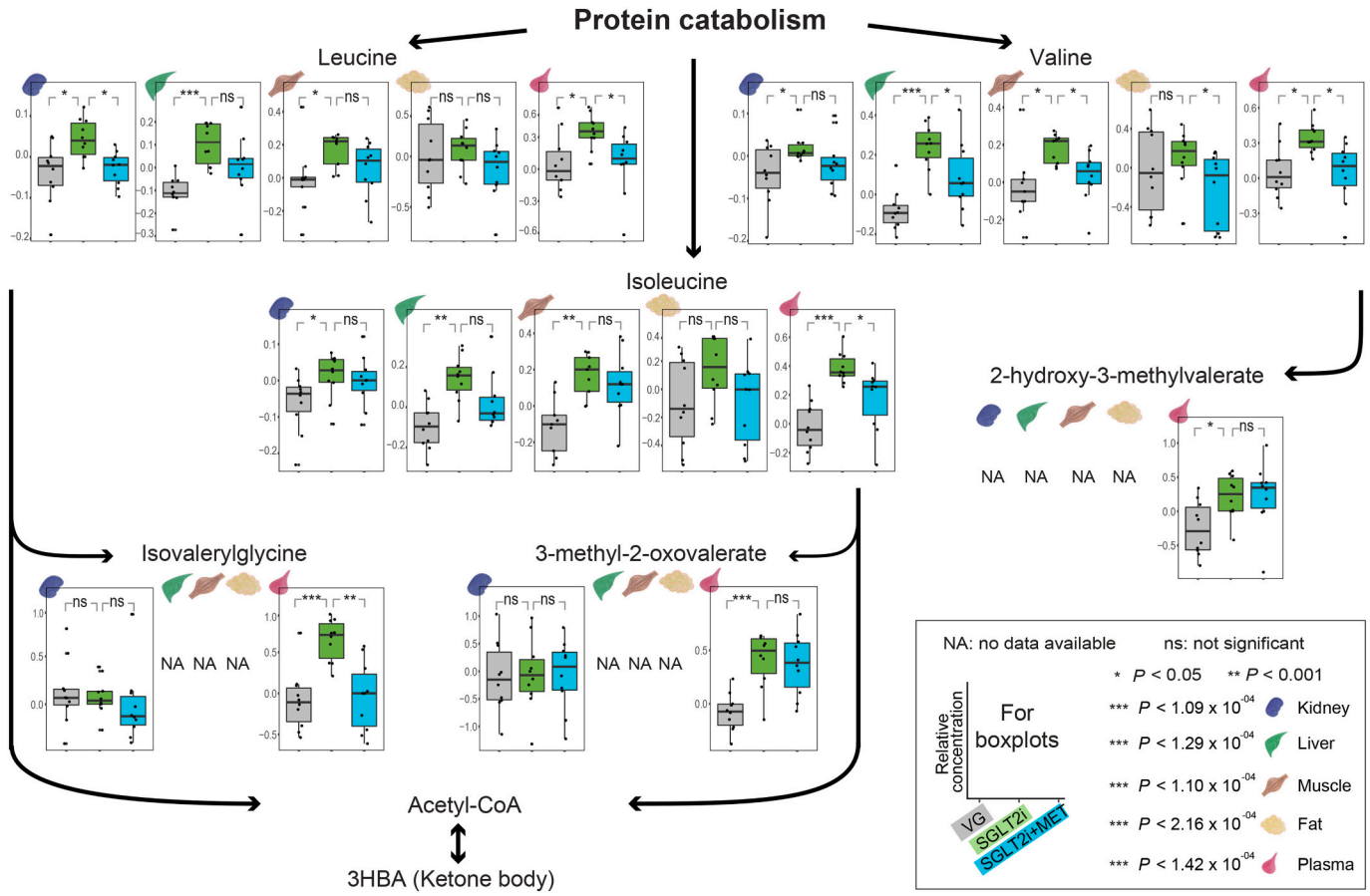

Fig. 4. BCAAs metabolism associated-metabolites in the five tissues.
Comparisons of the relative concentration of the branched-chain amino acids (BCAAs, leucine, isoleucine, and valine) metabolism-associated metabolites presented as boxplots in the kidney, liver, muscle, fat, and plasma among VG, SGLT2i and SGLT2i + MET mice. Abbreviations: HFD, high-fat diet; MET, metformin-treated db/db mice; NA, not available; ns; not significant; SGLT2i, SGLT2 inhibitor-treated db/db mice; SGLT2i + MET, SGLT2 inhibitor and metformin-treated db/db mice; VG, vehicle-gavaged db/db mice.

as DKA, but may also alleviate the risk associated with metformin monotherapy, namely lactic acidosis.

One of the key findings of our study is that 3HBA levels are significantly higher across all five tissues in mice treated with SGLT2i monotherapy, indicating activation of tissue-specific metabolic pathways (Fig. 5A). The metabolite 3HBA is one of the most abundant ketone bodies, predominantly produced from fatty acid oxidation-derived acetyl-coenzyme A (CoA) through hepatic ketogenesis during periods of caloric restriction (e.g., fasting). Our observation of higher levels of fatty acids suggests that SGLT2i monotherapy promoted hepatic fatty acid oxidation (Figs. 3B, 5A). Ketone body's metabolism plays a central role in physiological homeostasis as a source of energy for extrahepatic tissues such as the brain, heart, muscle, or kidney, and functions as a direct modulator of intracellular nutrient signals [30–33]. 3HBA was found to suppress glycogen synthase kinase (GSK) 3β and resulted in improved outcomes in terms of albuminuria and diabetic kidney disease in a murine model (Fig. 6A) [30]. In addition, it has been shown to suppress GSK3α [34]. It is widely recognized that the inhibition of GSK3β and GSK3α promotes glycogen synthase in liver and muscle [35,36]. However, it has been reported that SGLT2 inhibitors can activate the expression of phosphorylated GSK3β in renal proximal tubular cells (Fig. 6A) [37]. Our findings indicate that mice treated with SGLT2i exhibited lower levels of glycogens, specifically maltotriose and maltotetraose, in the liver (Fig. 3A). This can be attributed to the SGLT2i-induced decrease in glucose levels, which subsequently leads to a reduction in insulin levels (Fig. 6A, Table 2). The decrease in insulin levels further enhances the activity of GSK3β and GSK3α [38]. As a consequence, the glycogen level in the liver decreases (Fig. 6A).

Growing evidence from recent studies has demonstrated that elevated ketone bodies resulting from SGLT2i have renoprotective effects. Our observation of raised 3HBA, attributed to enhanced lipolysis and protein catabolism, including the metabolism of ketogenic amino acids, by SGLT2i monotherapy, provides additional support to the systemic organ protective mechanisms of the inhibitor. Tomita et al. reported that SGLT2i led to an increase in the concentration of ketone bodies, which subsequently inhibited mechanistic target of rapamycin complex 1 (mTOR1) in the kidney [32]. mTOR1-associated epithelial injury in the glomeruli was attenuated by ketone supplementation, and SGLT2i-treated mice and ketone supplementation significantly prevented tubulointerstitial fibrosis, inflammation, and apoptosis of proximal tubular epithelial cells [32].

Despite the potential benefits of the inhibitor of SGLT2, it is important to recognize that SGLT2i monotherapy can also have adverse effects. SGLT2i may lead to excessive progression of the protein catabolism and lipolysis, resulting in skeletal muscle loss and significant body weight loss, particularly in non-obese patients [11,12]. Given the global trend of an aging society and the increasing prevalence of elderly patients with T2D, it becomes important to address the physical challenges faced by this population, such as muscle weakness and sarcopenia [39,40]. T2D can further exacerbate these physical dysfunctions [39,41,42]. Therefore, it is necessary to find treatments that do not contribute to muscle weakness and sarcopenia, especially in elderly patients with T2D. Several previous studies have investigated changes in body composition after SGLT2i therapy [11,12]. These studies have

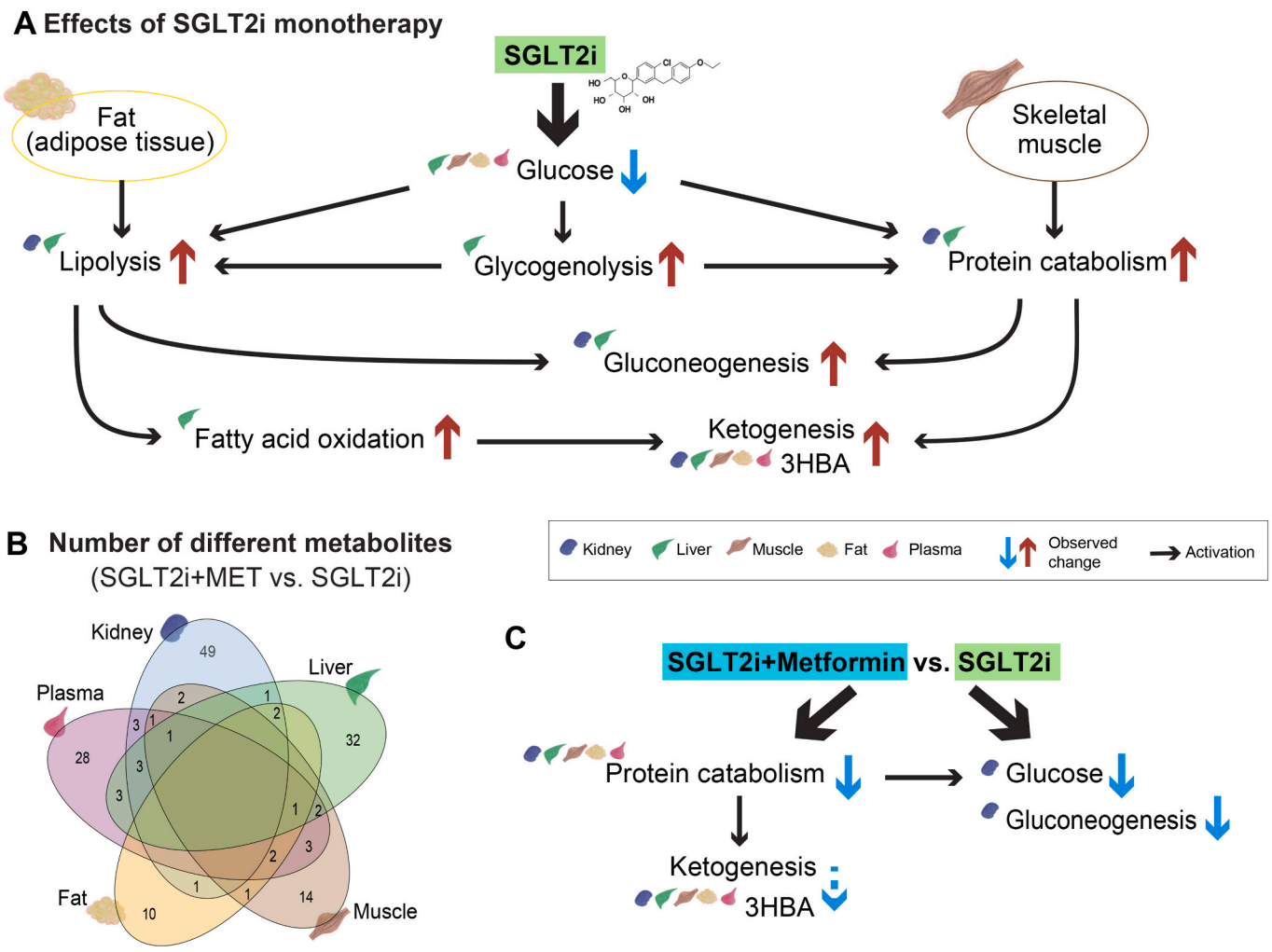

Fig. 5. Effects of SGLT2i monotherapy and combination with metformin on systemic metabolic pathways.
(A) Effects of SGLT2i monotherapy on the systemic metabolic pathways. (B) Number of metabolites significantly different when compared SGLT2i + MET to SGLT2i. (C) Effects of SGLT2i and metformin combination therapy compared with SGLT2i monotherapy on the systemic metabolic pathways.

indicated that SGLT2i therapy can lead to changes not only in body weight and fat mass, but also in muscle mass.

In the present study, we have shown that SGLT2i and metformin combination therapy may attenuate the adverse effects of SGLT2i or metformin monotherapy (Fig. 6B). We observed that the combination therapy attenuated levels of the ketone body in all five tissues, as well as metabolites associated with the protein catabolism, and gluconeogenesis in the kidney when compared to SGLT2i monotherapy (Fig. 5A, B). Our study provides additional evidence that the combination therapy may have a potential benefit in reducing the risk of DKA. The use of SGLT2i can cause DKA which is characterized by a functional state of starvation associated with excessive production and accumulation of ketones [10]. The U.S. Food and Drug Administration has previously issued a warning regarding the potential risk of euglycemic ketoacidosis associated with SGLT2i use and a total of 73 cases of ketoacidosis in patients with diabetes using SGLT2i have been reported [10]. Our observation of attenuated levels of systemic ketone body in the combination therapy may be due to the reduction in protein catabolism and the consequent ketogenic amino acid metabolism (Fig. 5C).

Overall, lactate levels were generally consistent across the four db/db mouse groups in all the examined tissues. An exception was noted in the plasma, where lactate levels were significantly lower in the group receiving combination therapy compared to the group treated with metformin alone (Table S5). This finding suggests that the risk of lactic acidosis could potentially be lower with the combination therapy than with metformin monotherapy, a hypothesis that gains support from the accompanying reduction in plasma levels of glucose and pyruvate, precursors to lactate, in the SGLT2i + MET group relative to the MET group (Fig. 6B, Table S5). These results imply that the combination of SGLT2i and metformin may exert a synergistic effect that not only enhances glycemic control but also reduces the substrate availability for lactate production, thereby possibly diminishing the likelihood of lactic acidosis.

The combination therapy may offer additional benefits beyond improved glycemic control, as we previously reported [19]. In the current study, we observed higher levels of pipecolate in kidney, liver, muscle, and plasma of mice treated with the combination therapy compared to those treated with SGLT2i monotherapy (Table S4). Pipecolate has been shown to possess antioxidant properties and promote extended cell survival in various cell lines and in vitro experiments, including HEK293 cells, RAW264.7 cells, oocytes, and myotubes [43–46]. These findings suggest that the increased levels of pipecolate resulting from combination therapy have multiple tissue-protective effects, including antioxidant, anti-inflammatory, and prolonged cell survival [43,47]. One mechanism through which pipecolate exerts its tissue-protective effects is by enhancing mTOR1 activity (Fig. 6A) [43,46]. Pipecolate can stimulate protein synthesis rates and influence lysine on protein turnover [46]. While mTOR1 inhibition by 3HBA in SGLT2i monotherapy can be beneficial, excessive inhibition of mTOR1 may have adverse effects. The combination therapy may help mitigate

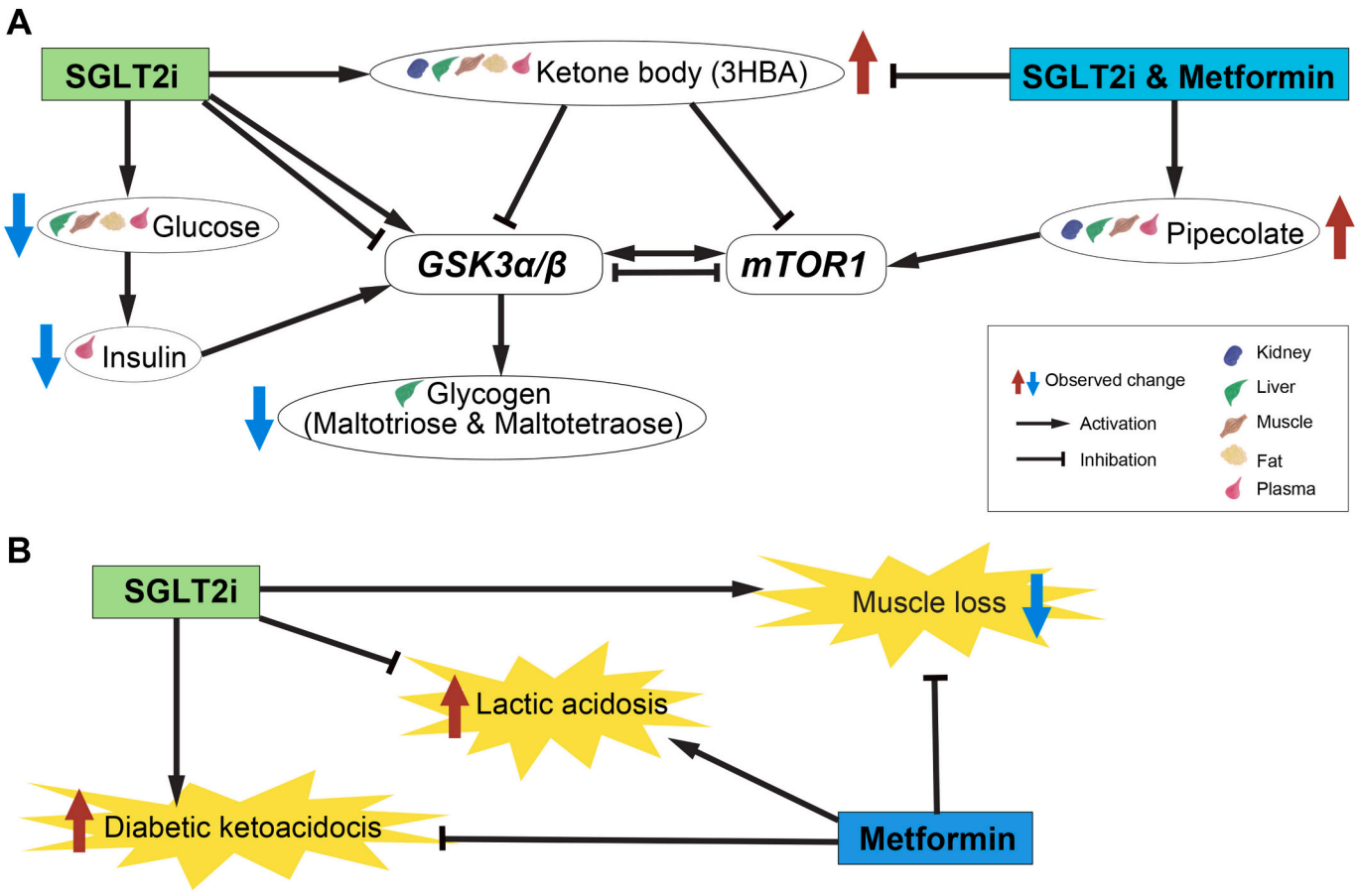

Fig. 6. Mechanism of action and the association between monotherapy and combination therapy.
(A) Potential molecular mechanisms and actions underlying the association between SGLT2i monotherapy and the combination therapy. (B) Adverse effects of SGLT2i and metformin monotherapy and the mechanisms of by which the combination therapy mitigates them. Abbreviations: GSK3, glycogen synthase kinase 3; mTOR1, mechanistic target of rapamycin complex 1.

these concerns by activating mTOR1 through increased pipecolate levels (Fig. 6A).

While we have previously highlighted the synergistic benefits of this combination therapy, it is indeed crucial to also consider its potential limitations. Notably, SGLT2i are known to offer cardioprotective effects through the activation of AMPK and SIRT1 pathways [48]. Metformin, which also activates AMPK, may potentially dampen the SGLT2i-dependent cardioprotective effects if AMPK is predominantly activated by metformin in the combination therapy [49]. Furthermore, a meta-analysis has indicated that combination therapy is associated with a doubled risk of genital infections and diarrhea when compared to the use of either metformin or SGLT2 inhibitors alone [50]. These considerations are important for the clinical management of patients receiving combined SGLT2i and metformin therapy.

The relationship between GSK3 and mTOR1 is intricate and varies across different tissues and cells. Previous research has shown that GSK3 can activate mTOR1 by phosphorylating the regulatory-associated protein of TOR, while it can also inhibit mTOR1 through the tuberous sclerosis complex 1/2 [51]. Conversely, mTOR1 can suppress GSK3 signaling in vitro [52]. Moreover, the close interaction between mTOR1 and GSK3 is associated with cell proliferation [53]. The cross-talk between GSK3 and mTOR1 may contribute to the phenotypic changes observed in various tissues of patients with T2D based on different treatments. Unraveling this complex issue represents a future challenge in this field.

A limitation of the current study was that we did not have data on changes in body composition. A long-term study is needed to determine the effect of SGLT2i monotherapy and its combination therapy with metformin in skeletal muscle.

In conclusion, SGLT2i monotherapy may lead to increased protein catabolism and higher 3HBA levels, potentially causing muscle loss over time. However, combining SGLT2i with metformin appears to mitigate this effect, lower the risk of diabetic DKA, and reduce the chance of metformin-associated lactic acidosis. Furthermore, the interaction between SGLT2i, metformin, and metabolic pathways involving GSK3 and mTORC1 suggests a complex mechanism that requires further investigation. Our findings imply that combination therapy could offer advantages over monotherapy, specifically in reducing muscle weakness, DKA, and lactic acidosis risks, but validation through studies with human data is needed.

Ethical statement

In this study, we performed the mice study using the C57BL6-based BKS.Cg-Dock7m+/+ Leprdb/J db/db mice. The mice were maintained in a specific pathogen-free facility and housed in a light- and temperature-controlled environment in compliance with FELASA (the Federation of Laboratory Animal Science Associations) protocols. Animal experiments were approved by the Upper Bavarian government (Gz.55.2-1-54-2531-70-07, 55.2-1-2532-153-11).

We did not utilize any human data in this study.

CRediT authorship contribution statement

Makoto Harada: Conceptualization, Formal analysis, Funding acquisition, Investigation, Visualization, Writing – original draft,

Writing – review & editing. **Siyu Han:** Formal analysis, Software. **Mengya Shi:** Formal analysis. **Jianhong Ge:** Investigation, Writing – review & editing. **Shixiang Yu:** Formal analysis. **Jonathan Adam:** Investigation. **Jerzy Adamski:** Methodology, Supervision. **Markus F. Scheerer:** Investigation, Methodology. **Susanne Neschen:** Investigation, Methodology, Project administration. **Martin Hrabe de Angelis:** Conceptualization, Funding acquisition, Resources, Supervision. **Rui Wang-Sattler:** Conceptualization, Funding acquisition, Investigation, Supervision, Visualization, Writing – original draft, Writing – review & editing.

Declaration of competing interest

Markus F. Scheerer was employed at Helmholtz Zentrum München during his PhD thesis and is currently employed in the CardioRenal Medical Department of Bayer AG, however, the company was not involved in work related to data and manuscript generation.

Susanne Neschen was employed by the Helmholtz Zentrum München during the execution of this study. She is currently an employee of Sanofi Aventis Deutschland GmbH, however, the company was not involved in work related to data and manuscript generation.

Data availability

Data will be made available on request.

Acknowledgments

We thank the Mouse200 project team of the German Mouse Clinic for excellent technical assistance (Babara Pfitzner, Alesia Walker and Gabriele Zieglmeier). We also appreciate the assistance with sample logistics and metabolomics measurements provided by the staff of the Genome Analysis Center Metabolomics Platform at the Helmholtz Zentrum München (Sven Zukunft).

Funding

Part of this study was supported by Uehara Memorial Foundation. This project has received funding from the Innovative Medicines Initiative 2 Joint Undertaking (JU) under grant agreement No. 821508 (CARDIATEAM). The JU receives support from the European Union's Horizon 2020 research and innovation programme and EFPIA. The German Diabetes Center is supported by the German Federal Ministry of Health (Berlin, Germany).

Appendix A. Supplementary data

Supplementary data to this article can be found online at https://doi.org/10.1016/j.ijbiomac.2024.130962.

References

[1] M.J. Davies, V.R. Aroda, B.S. Collins, R.A. Gabbay, J. Green, N.M. Maruthur, S. E. Rosas, S. Del Prato, C. Mathieu, G. Mingrone, P. Rossing, T. Tankova, A. Tsapas, J.B. Buse, Management of Hyperglycemia in Type 2 Diabetes, A consensus report by the American Diabetes Association (ADA) and the European Association for the Study of diabetes (EASD), Diabetes Care 45 (2022) (2022) 2753–2786, https://doi.org/10.2337/dci22-0034.

[2] J. Huang, C. Huth, M. Covic, M. Troll, J. Adam, S. Zukunft, C. Prehn, L. Wang, J. Nano, M.F. Scheerer, S. Neschen, G. Kastenmüller, K. Suhre, M. Laxy, F. Schliess, C. Gieger, J. Adamski, M. Hrabe de Angelis, A. Peters, R. Wang-Sattler, Machine learning approaches reveal metabolic signatures of incident chronic kidney disease in individuals with prediabetes and type 2 diabetes, Diabetes 69 (2020) 2756–2765, https://doi.org/10.2337/db20-0586.

[3] S. Abbas, S.T. Raza, F. Ahmed, A. Ahmad, S. Rizvi, F. Mahdi, Association of genetic polymorphism of PPARγ-2, ACE, MTHFR, FABP-2 and FTO genes in risk prediction of type 2 diabetes mellitus, J. Biomed. Sci. 20 (2013) 80, https://doi.org/10.1186/1423-0127-20-80.

[4] R.A. DeFronzo, E. Ferrannini, L. Groop, R.R. Henry, W.H. Herman, J.J. Holst, F. B. Hu, C.R. Kahn, I. Raz, G.I. Shulman, D.C. Simonson, M.A. Testa, R. Weiss, Type 2 diabetes mellitus, Nat. Rev. Dis. Primers 1 (2015) 15019, https://doi.org/10.1038/nrdp.2015.19.

[5] Y. Yu, Y. Xia, G. Liang, Exploring novel lead scaffolds for SGLT2 inhibitors: insights from machine learning and molecular dynamics simulations, Int. J. Biol. Macromol. 263 (2024) 130375, https://doi.org/10.1016/j.ijbiomac.2024.130375.

[6] J.M. Dennis, K.G. Young, A.P. McGovern, B.A. Mateen, S.J. Vollmer, M.D. Simpson, W.E. Henley, R.R. Holman, N. Sattar, E.R. Pearson, A.T. Hattersley, A.G. Jones, B. M. Shields, MASTERMIND consortium, Development of a treatment selection algorithm for SGLT2 and DPP-4 inhibitor therapies in people with type 2 diabetes: a retrospective cohort study, Lancet Digit. Health 4 (2022) e873–e883, https://doi.org/10.1016/S2589-7500(22)00174-1.

[7] G. Carney, J.D. Kim, C. O'Sullivan, W. Thompson, K. Bassett, J. Levin, C. R. Dormuth, Treatment pattern trends of medications for type 2 diabetes in British Columbia, Canada, BMJ Open Diabetes Res. Care 10 (2022) e002995, https://doi.org/10.1136/bmjdrc-2022-002995.

[8] A.A. Nargesi, G.P. Jeyashanmugaraja, N. Desai, K. Lipska, H. Krumholz, R. Khera, Contemporary national patterns of eligibility and use of novel cardioprotective antihyperglycemic agents in type 2 diabetes mellitus, J. Am. Heart Assoc. 10 (2021) e021084, https://doi.org/10.1161/JAHA.121.021084.

[9] E. Osto, F. Bonacina, A. Pirillo, G.D. Norata, Neutral effect of SGLT2 inhibitors on lipoprotein metabolism: from clinical evidence to molecular mechanisms, Pharmacol. Res. 188 (2023) 106667, https://doi.org/10.1016/j.phrs.2023.106667.

[10] H. Qiu, A. Novikov, V. Vallon, Ketosis and diabetic ketoacidosis in response to SGLT2 inhibitors: basic mechanisms and therapeutic perspectives, Diabetes Metab. Res. Rev. 33 (2017), https://doi.org/10.1002/dmrr.2886.

[11] J. Bolinder, Ö. Ljunggren, J. Kullberg, L. Johansson, J. Wilding, A.M. Langkilde, J. Sugg, S. Parikh, Effects of dapagliflozin on body weight, total fat mass, and regional adipose tissue distribution in patients with type 2 diabetes mellitus with inadequate glycemic control on metformin, J. Clin. Endocrinol. Metab. 97 (2012) 1020–1031, https://doi.org/10.1210/jc.2011-2260.

[12] A. Ohta, H. Kato, S. Ishii, Y. Sasaki, Y. Nakamura, T. Nakagawa, Y. Nagai, Y. Tanaka, Ipragliflozin, a sodium glucose co-transporter 2 inhibitor, reduces intrahepatic lipid content and abdominal visceral fat volume in patients with type 2 diabetes, Expert. Opin. Pharmacother. 18 (2017) 1433–1438, https://doi.org/10.1080/14656566.2017.1363888.

[13] B.A. Kappel, M. Lehrke, K. Schütt, A. Artati, J. Adamski, C. Lebherz, N. Marx, Effect of Empagliflozin on the metabolic signature of patients with type 2 diabetes mellitus and cardiovascular disease, Circulation 136 (2017) 969–972, https://doi.org/10.1161/CIRCULATIONAHA.117.029166.

[14] B.A. Kappel, J. Moellmann, K. Thiele, M. Rau, A. Artati, J. Adamski, B. Ghesquiere, K. Schuett, F. Romeo, R. Stoehr, N. Marx, M. Federici, M. Lehrke, Human and mouse non-targeted metabolomics identify 1,5-anhydroglucitol as SGLT2-dependent glycemic marker, Clin. Transl. Med. 11 (2021) e470, https://doi.org/10.1002/ctm2.470.

[15] R. DeFronzo, G.A. Fleming, K. Chen, T.A. Bicsak, Metformin-associated lactic acidosis: current perspectives on causes and risk, Metabolism 65 (2016) 20–29, https://doi.org/10.1016/j.metabol.2015.10.014.

[16] F.F. Richy, M. Sabidó-Espin, S. Guedes, F.A. Corvino, U. Gottwald-Hostalek, Incidence of lactic acidosis in patients with type 2 diabetes with and without renal impairment treated with metformin: a retrospective cohort study, Diabetes Care 37 (2014) 2291–2295, https://doi.org/10.2337/dc14-0464.

[17] E. Capobianco, Systems and precision medicine approaches to diabetes heterogeneity: a Big Data perspective, Clin. Transl. Med. 6 (2017) 23, https://doi.org/10.1186/s40169-017-0155-4.

[18] M. Bickel, H. Brummerhop, W. Frick, H. Glombik, A.W. Herling, H.O. Heuer, O. Plettenburg, S. Theis, U. Werner, W. Kramer, Effects of AVE2268, a substituted glycopyranoside, on urinary glucose excretion and blood glucose in mice and rats, Arzneimittelforschung 58 (2008) 574–580, https://doi.org/10.1055/s-0031-1296559.

[19] S. Neschen, M. Scheerer, A. Seelig, P. Huypens, J. Schultheiss, M. Wu, W. Wurst, B. Rathkolb, K. Suhre, E. Wolf, J. Beckers, M. Hrabé de Angelis, Metformin supports the antidiabetic effect of a sodium glucose cotransporter 2 inhibitor by suppressing endogenous glucose production in diabetic mice, Diabetes 64 (2015) 284–290, https://doi.org/10.2337/db14-0393.

[20] J. Adam, S. Brandmaier, J. Leonhardt, M.F. Scheerer, R.P. Mohney, T. Xu, J. Bi, M. Rotter, M. Troll, S. Chi, M. Heier, C. Herder, W. Rathmann, G. Giani, J. Adamski, T. Illig, K. Strauch, Y. Li, C. Gieger, A. Peters, K. Suhre, D. Ankerst, T. Meitinger, M. Hrabē de Angelis, M. Roden, S. Neschen, G. Kastenmüller, R. Wang-Sattler, Metformin effect on nontargeted metabolite profiles in patients with type 2 diabetes and in multiple murine tissues, Diabetes 65 (2016) 3776–3785, https://doi.org/10.2337/db16-0512.

[21] J. Huang, M. Covic, C. Huth, M. Rommel, J. Adam, S. Zukunft, C. Prehn, L. Wang, J. Nano, M.F. Scheerer, S. Neschen, G. Kastenmüller, C. Gieger, M. Laxy, F. Schliess, J. Adamski, K. Suhre, M.H. de Angelis, A. Peters, R. Wang-Sattler, Validation of candidate phospholipid biomarkers of chronic kidney disease in hyperglycemic individuals and their organ-specific exploration in leptin receptor-deficient db/db mouse, Metabolites 11 (2021) 89, https://doi.org/10.3390/metabo11020089.

[22] A.M. Evans, C.D. DeHaven, T. Barrett, M. Mitchell, E. Milgram, Integrated, nontargeted ultrahigh performance liquid chromatography/electrospray ionization tandem mass spectrometry platform for the identification and relative quantification of the small-molecule complement of biological systems, Anal. Chem. 81 (2009) 6656–6667, https://doi.org/10.1021/ac901536h.

[23] T. Ohta, N. Masutomi, N. Tsutsui, T. Sakairi, M. Mitchell, M.V. Milburn, J.A. Ryals, K.D. Beebe, L. Guo, Untargeted metabolomic profiling as an evaluative tool of

fenofibrate-induced toxicology in Fischer 344 male rats, Toxicol. Pathol. 37 (2009) 521–535, https://doi.org/10.1177/0192623309336152.
[24] E. Albrecht, M. Waldenberger, J. Krumsiek, A.M. Evans, U. Jeratsch, M. Breier, J. Adamski, W. Koenig, S. Zeilinger, C. Fuchs, N. Klopp, F.J. Theis, H.-E. Wichmann, K. Suhre, T. Illig, K. Strauch, A. Peters, C. Gieger, G. Kastenmüller, A. Doering, C. Meisinger, Metabolite profiling reveals new insights into the regulation of serum urate in humans, Metabolomics Off. J. Metabolomic Soc. 10 (2014) 141–151, https://doi.org/10.1007/s11306-013-0565-2.
[25] S. Han, J. Huang, F. Foppiano, C. Prehn, J. Adamski, K. Suhre, Y. Li, G. Matullo, F. Schliess, C. Gieger, A. Peters, R. Wang-Sattler, TIGER: technical variation elimination for metabolomics data using ensemble learning architecture, Brief. Bioinform. 23 (2022) bbab535, https://doi.org/10.1093/bib/bbab535.
[26] S. van Buuren, K. Groothuis-Oudshoorn, Mice: multivariate imputation by chained equations in R, J. Stat. Softw. 45 (2011) 1–67, https://doi.org/10.18637/jss.v045.i03.
[27] M. Shi, S. Han, K. Klier, G. Fobo, C. Montrone, S. Yu, M. Harada, A.-K. Henning, N. Friedrich, M. Bahls, M. Dörr, M. Nauck, H. Völzke, G. Homuth, H.J. Grabe, C. Prehn, J. Adamski, K. Suhre, W. Rathmann, A. Ruepp, J. Hertel, A. Peters, R. Wang-Sattler, Identification of candidate metabolite biomarkers for metabolic syndrome and its five components in population-based human cohorts, Cardiovasc. Diabetol. 22 (2023) 141, https://doi.org/10.1186/s12933-023-01862-z.
[28] D.S. Wishart, D. Tzur, C. Knox, R. Eisner, A.C. Guo, N. Young, D. Cheng, K. Jewell, D. Arndt, S. Sawhney, C. Fung, L. Nikolai, M. Lewis, M.-A. Coutouly, I. Forsythe, P. Tang, S. Shrivastava, K. Jeroncic, P. Stothard, G. Amegbey, D. Block, D.D. Hau, J. Wagner, J. Miniaci, M. Clements, M. Gebremedhin, N. Guo, Y. Zhang, G. E. Duggan, G.D. Macinnis, A.M. Weljie, R. Dowlatabadi, F. Bamforth, D. Clive, R. Greiner, L. Li, T. Marrie, B.D. Sykes, H.J. Vogel, L. Querengesser, HMDB: the human metabolome database, Nucleic Acids Res. 35 (2007) D521–D526, https://doi.org/10.1093/nar/gkl923.
[29] M. Kanehisa, S. Goto, Y. Sato, M. Kawashima, M. Furumichi, M. Tanabe, Data, information, knowledge and principle: back to metabolism in KEGG, Nucleic Acids Res. 42 (2014) D199–D205, https://doi.org/10.1093/nar/gkt1076.
[30] P. Puchalska, P.A. Crawford, Multi-dimensional roles of ketone bodies in fuel metabolism, signaling, and therapeutics, Cell Metab. 25 (2017) 262–284, https://doi.org/10.1016/j.cmet.2016.12.022.
[31] Y. Mizuno, E. Harada, H. Nakagawa, Y. Morikawa, M. Shono, F. Kugimiya, M. Yoshimura, H. Yasue, The diabetic heart utilizes ketone bodies as an energy source, Metabolism 77 (2017) 65–72, https://doi.org/10.1016/j.metabol.2017.08.005.
[32] I. Tomita, S. Kume, S. Sugahara, N. Osawa, K. Yamahara, M. Yasuda-Yamahara, N. Takeda, M. Chin-Kanasaki, T. Kaneko, E. Mayoux, M. Mark, M. Yanagita, H. Ogita, S.-I. Araki, H. Maegawa, SGLT2 inhibition mediates protection from diabetic kidney disease by promoting ketone body-induced mTORC1 inhibition, Cell Metab. 32 (2020) 404–419.e6, https://doi.org/10.1016/j.cmet.2020.06.020.
[33] A.P. Koutnik, D.P. D'Agostino, B. Egan, Anticatabolic effects of ketone bodies in skeletal muscle, Trends Endocrinol Metab 30 (2019) 227–229, https://doi.org/10.1016/j.tem.2019.01.006.
[34] L. Ortega-Paz, H. Cristóbal, J.T. Ortiz-Perez, P. García de Frutos, G. Mendieta, E. Sandoval, J.J. Rodriguez, E. Ortega, A. García-Álvarez, S. Brugaletta, M. Sabaté, A.P. Dantas, Direct actions of dapagliflozin and interactions with LCZ696 and spironolactone on cardiac fibroblasts of patients with heart failure and reduced ejection fraction, ESC Heart Fail. 10 (2023) 453–464, https://doi.org/10.1002/ehf2.14186.
[35] K. MacAulay, B.W. Doble, S. Patel, T. Hansotia, E.M. Sinclair, D.J. Drucker, A. Nagy, J.R. Woodgett, Glycogen synthase kinase 3alpha-specific regulation of murine hepatic glycogen metabolism, Cell Metab. 6 (2007) 329–337, https://doi.org/10.1016/j.cmet.2007.08.013.
[36] G.W. Cline, K. Johnson, W. Regittnig, P. Perret, E. Tozzo, L. Xiao, C. Damico, G. I. Shulman, Effects of a novel glycogen synthase kinase-3 inhibitor on insulin-stimulated glucose metabolism in Zucker diabetic fatty (fa/fa) rats, Diabetes 51 (2002) 2903–2910, https://doi.org/10.2337/diabetes.51.10.2903.
[37] V. Mihaljević, M. Zjalić, T. Kizivat, T. Omanović Kolarić, M. Smolić, E. Rođak, M. Čović, L. Kuna, R. Smolić, A. Včev, I. Bilić Ćurčić, Molecular mechanisms linking empagliflozin to renal protection in the LLC-PK1 model of diabetic nephropathy, Biomedicines 10 (2022) 2983, https://doi.org/10.3390/biomedicines10112983.
[38] D.A. Cross, D.R. Alessi, P. Cohen, M. Andjelkovich, B.A. Hemmings, Inhibition of glycogen synthase kinase-3 by insulin mediated by protein kinase B, Nature 378 (1995) 785–789, https://doi.org/10.1038/378785a0.
[39] A.J. Cruz-Jentoft, A.A. Sayer, Sarcopenia, Lancet Lond. Engl. 393 (2019) 2636–2646, https://doi.org/10.1016/S0140-6736(19)31138-9.
[40] S. Chatterjee, K. Khunti, M.J. Davies, Type 2 diabetes, Lancet Lond. Engl. 389 (2017) 2239–2251, https://doi.org/10.1016/S0140-6736(17)30058-2.
[41] S.W. Park, B.H. Goodpaster, E.S. Strotmeyer, N. de Rekeneire, T.B. Harris, A. V. Schwartz, F.A. Tylavsky, A.B. Newman, Decreased muscle strength and quality in older adults with type 2 diabetes: the health, aging, and body composition study, Diabetes 55 (2006) 1813–1818, https://doi.org/10.2337/db05-1183.
[42] Y. Hashimoto, F. Takahashi, T. Okamura, M. Hamaguchi, M. Fukui, Diet, exercise, and pharmacotherapy for sarcopenia in people with diabetes, Metabolism 144 (2023) 155585, https://doi.org/10.1016/j.metabol.2023.155585.
[43] S.K. Natarajan, E. Muthukrishnan, O. Khalimonchuk, J.L. Mott, D.F. Becker, Evidence for pipecolate oxidase in mediating protection against hydrogen peroxide stress, J. Cell. Biochem. 118 (2017) 1678–1688, https://doi.org/10.1002/jcb.25825.
[44] S. Nishitani, A. Fukuhara, Y. Jinno, H. Kawano, T. Yano, M. Otsuki, I. Shimomura, Metabolomic analysis of diet-induced obese mice supplemented with eicosapentaenoic acid, Exp. Clin. Endocrinol. Diabetes Off. J. Ger. Soc. Endocrinol. Ger. Diabetes Assoc. 128 (2020) 548–555, https://doi.org/10.1055/a-0802-9064.
[45] T. Treleaven, M.L.M. Hardy, M. Guttman-Jones, M.B. Morris, M.L. Day, In vitro fertilisation of mouse oocytes in L-proline and L-pipecolic acid improves subsequent development, Cells 10 (2021) 1352, https://doi.org/10.3390/cells10061352.
[46] T. Sato, Y. Ito, T. Nagasawa, Regulatory effects of the L-lysine metabolites, L-2-aminoadipic acid and L-pipecolic acid, on protein turnover in C2C12 myotubes, Biosci. Biotechnol. Biochem. 80 (2016) 2168–2175, https://doi.org/10.1080/09168451.2016.1210499.
[47] N. Krishnan, M.B. Dickman, D.F. Becker, Proline modulates the intracellular redox environment and protects mammalian cells against oxidative stress, Free Radic. Biol. Med. 44 (2008) 671–681, https://doi.org/10.1016/j.freeradbiomed.2007.10.054.
[48] M. Packer, SGLT2 inhibitors produce cardiorenal benefits by promoting adaptive cellular reprogramming to induce a state of fasting mimicry: a paradigm shift in understanding their mechanism of action, Diabetes Care 43 (2020) 508–511, https://doi.org/10.2337/dci19-0074.
[49] M. Packer, Does metformin interfere with the cardiovascular benefits of SGLT2 inhibitors? Questions about its role as the cornerstone of diabetes treatment, Am. J. Med. 133 (2020) 781–782, https://doi.org/10.1016/j.amjmed.2020.01.016.
[50] T.Y. Milder, S.L. Stocker, C. Abdel Shaheed, L. McGrath-Cadell, D. Samocha-Bonet, J.R. Greenfield, R.O. Day, Combination therapy with an SGLT2 inhibitor as initial treatment for type 2 diabetes: a systematic review and meta-analysis, J. Clin. Med. 8 (2019) 45, https://doi.org/10.3390/jcm8010045.
[51] C. Evangelisti, F. Chiarini, F. Paganelli, S. Marmiroli, A.M. Martelli, Crosstalks of GSK3 signaling with the mTOR network and effects on targeted therapy of cancer, Biochim. Biophys. Acta, Mol. Cell Res. 1867 (2020) 118635, https://doi.org/10.1016/j.bbamcr.2019.118635.
[52] L. He, A.P. Gomes, X. Wang, S.O. Yoon, G. Lee, M.J. Nagiec, S. Cho, A. Chavez, T. Islam, Y. Yu, J.M. Asara, B.Y. Kim, J. Blenis, mTORC1 promotes metabolic reprogramming by the suppression of GSK3-dependent Foxk1 phosphorylation, Mol. Cell 70 (2018) 949–960.e4, https://doi.org/10.1016/j.molcel.2018.04.024.
[53] M. Ka, G. Condorelli, J.R. Woodgett, W.-Y. Kim, mTOR regulates brain morphogenesis by mediating GSK3 signaling, Dev. Camb. Engl. 141 (2014) 4076–4086, https://doi.org/10.1242/dev.108282.